

MICROMECHANICAL BEHAVIOR OF FRP COMPOSITES WITH HIGRO-THERMAL DAMAGE

Nestor D. Barulich^a, Luis A. Godoy^b, Patricia M. Dardati^a

^a *Universidad Tecnológica Nacional, Facultad Regional Córdoba. Maestro M. Lopez esq. Cruz Roja Argentina, Córdoba 5000, Argentina, dariobarulich@hotmail.com, pdardati@industrial.frc.utn.edu.ar, <http://www.frc.utn.edu.ar>*

^b *Universidad Nacional de Córdoba, Facultad de Ciencias Exactas, Físicas y Naturales, Departamento de Estructuras, Avenida Vélez Sarsfield 1611, Córdoba 5000, Argentina. lgodoy@com.uncor.edu, <http://www.efn.uncor.edu>*

Keywords: Composite material, Higo-thermal damage, Finite elements.

Abstract. The stress field in a representative volume element (RVE) of a composite material formed by e-glass fibers and polymer matrix is investigated. The assumed RVE is a regular domain in plane strain, including 25 fibers and under a shear load field. Damage in the form of interface debonding is included in the model, in order to represent damage due to higo-thermal action (not produced by mechanical loads). The specific form of damage follows micrographs obtained in experiments, from which debonding may be approximated as a shallow ellipse. The redistributions of stresses is investigated using a finite element representation of the RVE using the general purpose finite element code ABAQUS. Both elastic and elasto-plastic models are studied in order to identify likely propagation patterns of the assumed initial damage. Parametric studies are reported by varying the extent of damage (length of the ellipse), the fiber volume fraction, and the number of fibers affected by damage. The results for elastic models show that damage at one interface affects the eight fibers in the neighborhood (a Moore neighborhood), four of which increase their stress levels and the other four (in diagonal with respect to the fiber affected) decrease their values. Results from elasto-plastic models indicate that the number of voids decreases the load at failure only if the voids are aligned.

1 INTRODUCTION

In applications in aggressive environments, composite materials may suffer from corrosion of degradation that eventually lead to failure. The specific mechanism by which damage occurs due to environmental factor is complex and must be initially evaluated using experiments. An experimental assessment to estimate potential damage under various environmental conditions is a slow and costly process, so that it is highly desirable to employ computational methods to perform modeling under representative conditions. Some researchers characterized degradations of the material properties at the macro level; however damage originates at the micro-structural level and there is great interest in understanding behavior at that level. A thorough understanding of the behavior of a composite with damage requires an investigation at the micro-level, which is where damage initiates and propagates up to macro levels (Godoy, 2003).

This paper reports results obtained from computational models of a composite including degradations of properties and damage by means of a representation of the micro-structure. There are at least two scales of analysis in this problem, one at the macro level, where the behavior of the composite is represented as an equivalent anisotropic and homogeneous material, and a scale at the micro-level, in which the laminate degradation at a layer may be studied in terms of a Representative Volume Element (RVE) or a Unit Cell (UC) (Jones, 1999). This work concentrates on the micromechanics of this problem in order to identify stress levels produced by damage at the fiber-matrix interface and its propagation.

2 LITERATURE REVIEW

In composites produced using e-glass and epoxy matrix, it is currently accepted that forms of damage may affect (i) the matrix, (ii) the fibers, or (iii) the interface between them. The occurrence of each depends on the constituent elements and on the type of adhesion that may be reached at the interface.

Regarding mechanisms of degradation, Kajorncheappunngam et al. (2002) immersed composite samples in four different liquids, with properties measured at ambient temperature and at 60°C. All the solutions analyzed produced degradation of the mechanical properties of the resin, especially at high temperatures. For samples immersed in an acid solution at ambient temperature (and also for alkaline solutions at elevated temperatures), the tensile strength of the composite was reduced by more than 70%. Ray (2005) investigated temperature effects during moisture aging at the interface, under constant water temperature.

Research on higo-thermal aging of composites by Foulc et al. (2005) identified four degradation stages in the composite: (i) Plasticity, (ii) chemical degradation, (iii) morphological evolution, (iv) interphase damage (debonding). This study identified that interphase damage mainly occurs due to void and crack formation; water absorption are induced by such damage and leads to fracture in the material. The experimental identification of higo-thermal damage has also been reported by Obando et al. (2009).

Regarding computational models, it is important to distinguish between phenomenological models and simulations of material behavior. Damage introduced in classical lamination theory (Jones, 1999) belongs to the first group, in which average properties are represented and local effects and damage are not taken into account. Reifsnider (1994) carried out simulations with detailed interphase models and considered various classes of strength and durability. Bonora and Rugiero (2005) considered a micro-mechanical model with mechanical interface, assuming various unit cell configurations for metal matrix composites. Damage was induced by means of strains, and had various forms, including fiber rupture, matrix damage and

matrix-interface separation. Three distinct phases were identified in the stress-strain curves: first, a linear elastic response in which fiber and matrix have perfect adhesion; second, there is a change in the slope with initial separation between constituent materials; third, a rapid increase in strain due to a small increase in stress. Micro-cracking initiates at this third stage, and is identified as the source of composite failure. Another micro-mechanical model was reported by [Caporale et al. \(2006\)](#), in which fiber and matrix are assumed as homogeneous, isotropic and elastic, and failure is possible at the fiber-matrix connection by introducing elasto-fragile springs. External loads or displacements were employed by these authors to induce stresses in the material. Degradation of material properties and micro-structure evolution of a fiber-reinforced thermo-plastic composite due to this effect has been investigated by [Sevostianov et al. \(2003\)](#), who concluded that damage accumulation produces changes in both, mechanical and thermal properties of the composite.

Computational as well as experimental research for a particle reinforced composite with mechanical damage was also carried out by [Kwon \(1997\)](#). The analytical model was based on one quarter of the unit cell with a void at the center of the particle.

Finally, the most relevant study for present purposes was presented by [Kaminski \(2005\)](#), who represented damage using semi-circular voids at unit cell level (modeling one quarter of the cell). Both the number of voids and their size were taken as parameters. This was followed by reports of [Godoy et al. \(2008\)](#) on complete unit cells along the lines of the present work.

3 METHODOLOGY

Rather than using unit cell domains, 2D Representative Volume Elements (RVE) have been considered in this work. The specific composite has unidirectional e-glass fibers in epoxy, under shear load. Higo-thermal damage is assumed in the form of debonding; such damage is not caused by mechanical loads.

Two models were used, covering elastic and ideal elasto-plastic material behavior. Computations under plane strain assumptions were carried out using the finite element package [ABAQUS \(2009\)](#).

The results are given in terms of von Mises equivalent stresses in a cross section that is normal to the direction of the fibers. A parametric study at RVE level is carried out to consider the influence of fiber volume fraction, number of fibers, and location and size of damage. As reference values, results for undamaged composites under six V_f values were computed. The elastic models are used to better understand stress redistributions in a RVE, whereas plasticity is used to visualize damage propagation and strength levels.

4 RVE MODEL

4.1 Geometry of the domain considered

Similar basic features were employed for damaged and undamaged cases using both material models. The specific RVE was assumed to have a regular pattern of equally spaced fibers located in a square grid, as shown in [Figure 1](#). The RVE includes 25 fibers, with unit separation between the centers of two adjacent fibers. It is also assumed that the domain does not change as a consequence of deformations of the solid, so that the location of fibers in space remain unmodified.

4.2 Boundary conditions

Assumed loads in the form of distributed shear are applied at the element boundaries.

Notice that shear has been identified to be the worse condition based on unit cell models (Godoy et al, 2008). Rigid body motions were eliminated by constraining the central point and one corner point of the RVE.

Unit load (1MPa) was used for the elastic model, but for the elasto-plastic model a load of 48.26 MPa was used, which corresponds to the yield value in the matrix. Solution of the equations was achieved by use of the Newton-Raphson method.

	E [MPa]	ν	σ_f [MPa]
Epoxi	4000	0.38	48.26
e-glass	84000	0.22	-

Table 1: Matrix and Fiber properties

V_f	d
0.3	0.618
0.5	0.798
0.6	0.874
0.65	0.909
0.7	0.944
0.75	0.977

Table 2: Fiber volume fraction and diameter

4.3 Material properties

Following Godoy et al. (2008), the mechanical properties assumed for matrix and fibers are shown in Table 1. In the initial analysis the materials are assumed to have elastic behavior. For the model with plasticity, it is assumed that the matrix behaves as an ideal elasto-plastic material with yield stress σ_f .

4.4 Damage model

As said before, higo-thermal damage is assumed as fiber-matrix debonding. Microscopy observations reported by Mondragón (2008) indicate that voids are induced at the interface, with the form of a shallow ellipse (see Figure 1). This type of representation has previously been used by Kaminski (2005) for damage due to mechanical origin. Damage size is given by the fraction of the fiber perimeter affected by the void, with a minimum value of 12.5% (an ellipse extending 45 degrees around the circumference) and a maximum of 50%.

4.5 Fiber volume fraction

Use Fiber volume fraction V_f is defined as the ratio between the fiber volume and the total volume of composite material. For a given depth in plane strain, the value is computed from a relation between areas, in the form:

$$V_f = \frac{\pi}{4} \left(\frac{d}{s} \right)^2 \quad (1)$$

where d is the diameter of fibers and s is the separation between centers of adjacent fibers. The values of V_f , which are indicated in Table 2 together with their diameters, were chosen based on electro-micrographs, in which no contact was observed between fibers. This model would have a maximum value of $V_f = \pi/4$ (contact between two fibers), but the maximum value for which computations were performed was $V_f = 0.75$.

4.6 Discretization

For the elastic model, a dense finite element mesh was built using 8-node quadrilaterals and 6-node triangles (identified as CPE8 and CPE6 in ABAQUS) under plane strain conditions. The zone of higher density of elements in the mesh may be seen in Figure 7 for a model with $V_f = 75\%$. For the elasto-plastic material, linear triangular elements (identified as CPE3 in ABAQUS) under plane strain were adopted.

5 ANALYSIS UNDER ELASTIC BEHAVIOR

5.1 Results for an undamaged RVE

The analysis of RVE without damage is discussed in this section. Results are presented in Figures 2 to 7, and they are summarized at specific cross sections in Figures 8 to 11. The nomenclature to identify a plot is, for example, as Vert 0 V_f 07, where “Vert” or “Horiz” indicate vertical or horizontal sections, “0” is the coordinate of the horizontal or vertical section measured with respect to a central reference system; and “ V_f 07” indicates the value of V_f .

The results have a periodic nature, except for a small section close to the edges of the RVE. Symmetry in von Mises stresses with respect to geometric lines of symmetry was obtained, with maximum value occurring at the matrix-fiber interface.

The stress concentration around a fiber increases with V_f , as shown in Figures 8, 9 and 11 with values of 2.3 MPa to 4.6 MPa for models with $V_f = 30\%$ and 75% respectively. A shift in maximum values is observed, which move from a location at 45° (indicated as Zoom 2 in Figures 2 and 3) towards locations closer to the vertical and horizontal lines (indicated as Zoom 3 in Figures 4, 5 and 6). In the model with $V_f = 30\%$ there are high stresses (although not a maximum) in the matrix away from the interface (Zoom 1); this is considerably reduced in other models.

5.2 Results for a RVE with damage

Results for various damage conditions assuming high-thermal damage are reported in this section. Because there is a singularity at the edges of the void, as shown in Figure 1, the maximum values at those locations are not discussed in the following.

5.2.1 Influence of damage size

For a composite with $V_f = 30\%$, damage with increasing size was investigated to understand the stress redistributions that occur. The plots have scales with limits given by maximum and minimum values computed in the undamaged configuration, i.e. 0.468 MPa and 2.36 MPa (Figures 12 to 16).

There is a clear increase in von Mises stresses at the interface of fibers identified as “A”, as shown in Figures 14 and 15: those are fibers located at what is known as a Dirichlet vicinity in cellular automata methodology. In fiber termed “B”, on the other hand, there is a reduction in the stress at the interface (see Zoom 1 in Figure 16), whereas fibers “C” do not have any

significant changes (see Zoom 2 in Figure 16). High stresses are always present at the interfaces of the domain.

5.2.2 Influence of fiber volume fraction

To appreciate changes that occur as a consequence of damage acting on various V_f configurations, the results are compared with undamaged models. The results in Figure 17 to 19 show stress scales corresponding to undamaged values.

The results indicate that an increase in V_f is accompanied by an increase in the maximum values of stresses and tend to align with the lines that join fiber centers (zones designated as “E” in Figures 18 and 19). Stresses in the matrix in zone “D”, on the other hand, show a decrease with an increase in V_f .

5.2.1 Influence of the number of fibers exhibiting damage

Based on the stress redistribution identified in Figure 17 to 19, damage was further introduced in order to investigate the influence of more widespread damage. It was decided to introduce damage at the center of the RVE, in order to avoid boundary effects.

The results of Figures 20 to 24 show increase of stresses at the interface with increasing number of fiber affected by damage. Worse configurations are detected whenever the distributions follows patterns as those shown in Figures 23 and 24, and the stress increase affects small zones of the domain (zones “G”).

6 ANALYSIS INCLUDING PLASTICITY

Failure loads Q_r reported in each case are given as a percentage of the matrix yield stress and are identified whenever there is plasticity along a line that joins the void and the boundary of the RVE (see Figures 25). In all cases it was verified that large strains at the RVE were computed for a small increment in the load. Failure was always obtained before the value of σ_f was reached.

6.1 Results for a RVE without damage

Plasticity initiates at the points of maximum von Mises stress, and failure occurs with plasticity levels affecting most of the matrix, as shown in Figure 26. Values of failure load for various values of fiber volume fraction are shown in Table 3. Notice that there are no significant differences among them.

		Failure Loads			
Case		Fiber Volume Fraction			
N°	Description	Vf=30%	Vf=50%	Vf=65%	Vf=75%
1	Undamaged	$Q_r=56\%$	$Q_r=56\%$	$Q_r=56\%$	$Q_r=57\%$
2	Damage 25%	$Q_r=55\%$	$Q_r=55\%$	$Q_r=55\%$	$Q_r=55\%$

Table 3: Failure load, for a RVE without damage and with damage at the center.

6.2 Results for RVE with damage

6.2.1 Influence of the fiber volume fraction

Results of failure loads for various fiber fractions are listed in Table 3. Such values are not significantly different from those obtained for an undamaged material. For the present orientation of damage, the extension of plastic zone occurs in the horizontal direction and plastic zones do not coalesce in other direction. For a void located as in Figure 27, the extension of plastic zone would occur in the vertical direction.

6.2.2 Influence of void size

Changes in damage size ranging between 12.5% and 50% were investigated for a RVE with $V_f=30\%$, and the results are listed in Table 4. However, there are no significant differences with the results for the second case in Table 3 for $V_f=30\%$.

Failure Loads		
Case		Fiber Volume Fraction
N°	Description	$V_f=30\%$
3	Damage 12.5%	$Q_r= 56\%$
4	Damage 50%	$Q_r= 55\%$

Table 4: Failure load for different damage size.

6.2.3 Influence of the number of fiber in which interphase damage occurs

Results computed for nine voids are shown in Table 5, and a reduction is observed in the load at failure. Propagation of damage occurs in this case following three horizontal lines towards the contour of the element (Figure 28).

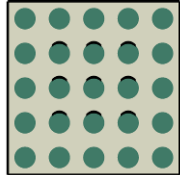
Failure Loads			
Case		Fiber Volume Fraction	
N°	Description	$V_f=30\%$	$V_f=75\%$
11	Nine voids 25% 	$Q_r= 45\%$	$Q_r= 40\%$

Table 5: Failure load with nine voids.

6.2.4 Influence of damage location

Values are summarized in Table 6, and by comparison with those of Table 3 it seems that there is no interaction among voids located at different rows, leading in all cases to the same failure load. Specifically, this results from comparisons of cases 5 and 7 in Table 6 with case 2 in Table 3, and comparisons of cases 6, 8, 9 in Table 6 ($V_f=75\%$).

Considering case 6 with two voids in the same horizontal row 3, and adding a new void in other row does not influence the load. It is concluded that there is no influence between voids that are not aligned. On the other hand, for the same case 6 with two voids, if a new void is placed aligned with the others, then there is a reduction in failure load.

Failure Loads			Case		
Case		Fiber Volume Fraction	Case		Fiber Volume Fraction
N°	Description	$V_f=75\%$	N°	Description	$V_f=75\%$
5		$Q_r= 55\%$	9		$Q_r= 47.5\%$
6	 Two voids 25%	$Q_r= 47.5\%$	10	 Three voids 25%	$Q_r= 46\%$
7	 Two voids oblique 25%	$Q_r= 55\%$	11	 Four voids 25%	$Q_r= 47.5\%$
8	 Three voids 25%	$Q_r= 47.5\%$	12	 Nine Voids 25%	$Q_r= 40\%$

Table 6: Failure load for a RVE with $V_f = 75\%$ for various damage configurations.

7 CONCLUSIONS

Results for Representative Volume Elements have been reported under various damage configurations, and some important conclusions may be drawn for future research. Most previous work in the literature was limited to unit cell models, in which just one fiber is included together with the surrounding matrix; however, this seems to provide only a limited view of the state of fibers that may be affected in the neighborhood. Our elastic results illustrate that damage at the interface affects a vicinity which is known in cellular automata as the Moore vicinity, which includes eight neighboring fibers. Fibers oriented as in the Dirichlet vicinity (those located in horizontal or vertical positions) have an increase in stress field, whereas those along diagonal lines experience reductions in the stresses, so that there is a stress redistribution. This is an important observation in order to develop cellular automata models of this problem, in which each fiber and its interface are modeled as an element in a grid.

The elasto-plastic model under shear shows that for a given damage, the fiber volume fraction does not modify the failure load. Further, the number of voids decreases the load at

failure only if they are aligned.

The results indicate that damage propagations should be studied at a Representative Volume Element, rather than using a more simplified Unit Cell representation of the micro-domain, as has been done in previous studies.

Acknowledgements: This work was supported by a grant of the Ministry of Science and Technology of the Province of Cordoba, in Argentina, titled: “Multi-scale analysis of forming and degradation processes in materials and structural components”. D. Barulich had a scholarship of the National Technological University during this research. L. Godoy is a member of the scientific staff of CONICET (Science & Technology Research Council of Argentina).

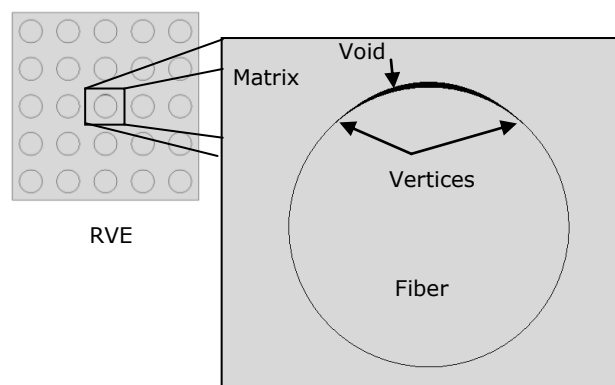


Figure 1: Damage representation by an interface void.

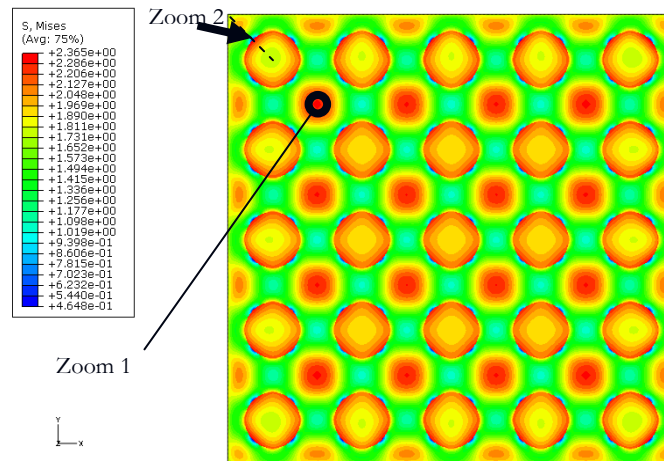


Figure 2: RVE with $V_f = 0.3$

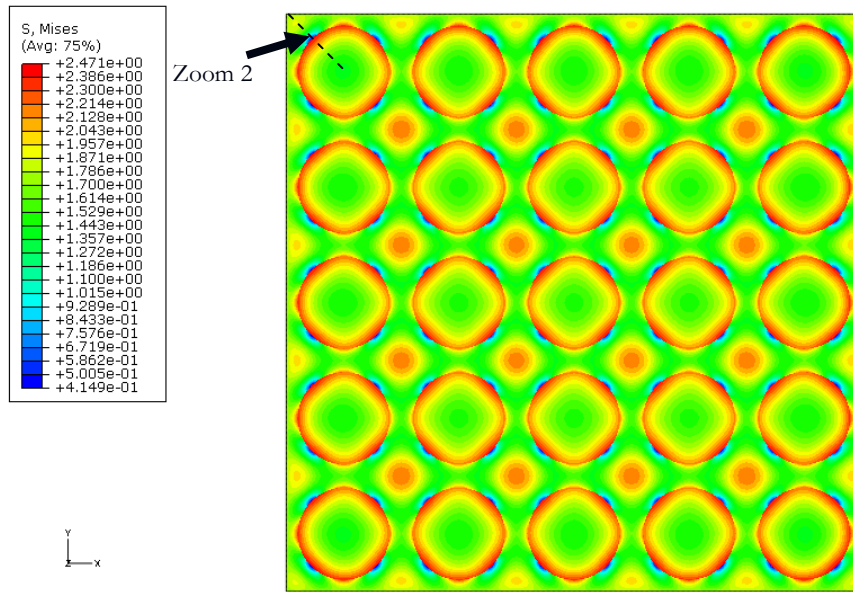


Figure 3: RVE with $V_f= 0.5$

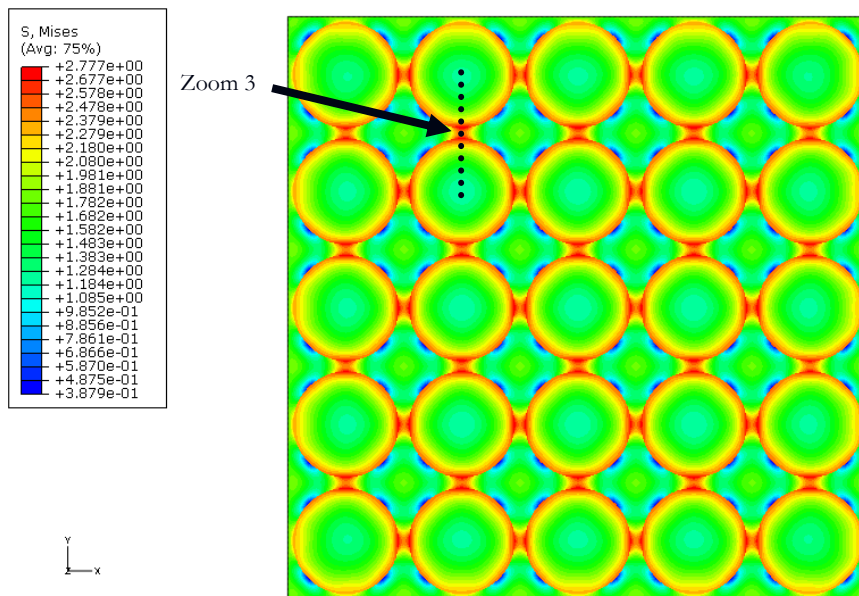


Figure 4: RVE with $V_f= 0.65$

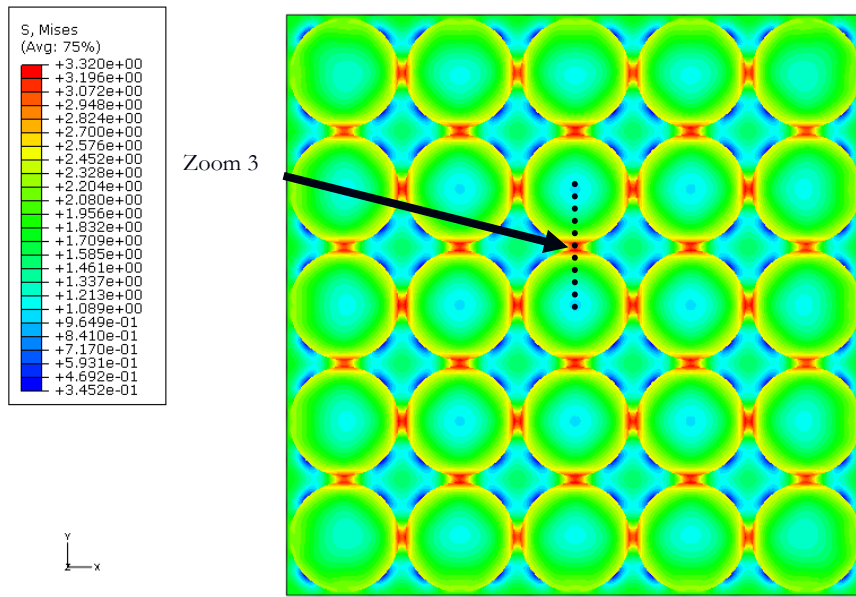


Figure 5: RVE with $V_f = 0.7$

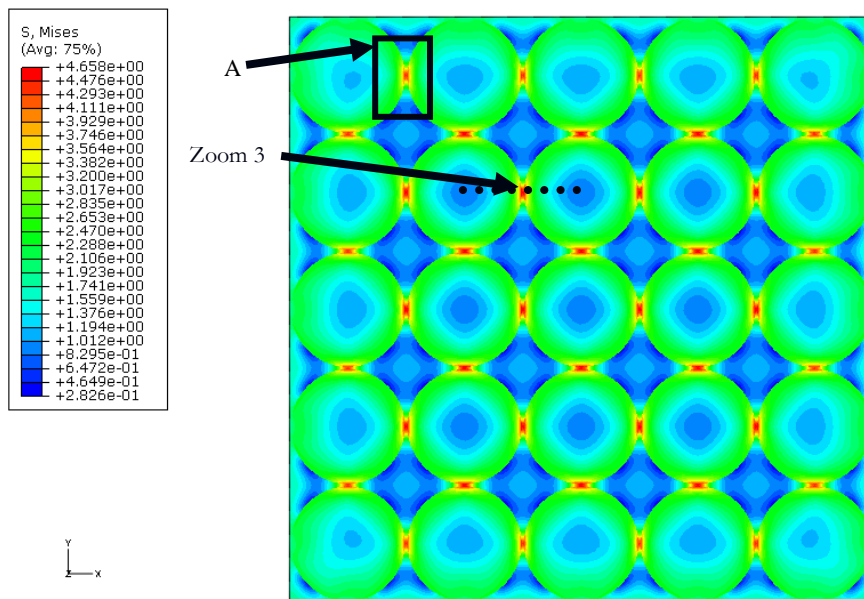


Figure 6: RVE with $V_f = 0.75$.

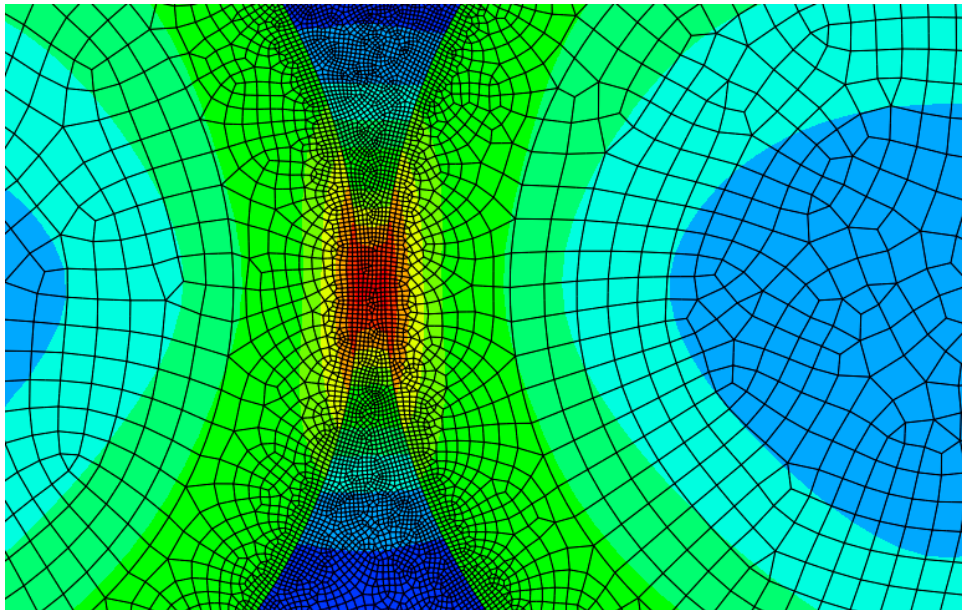


Figure 7: Zoom A in Figure 6.

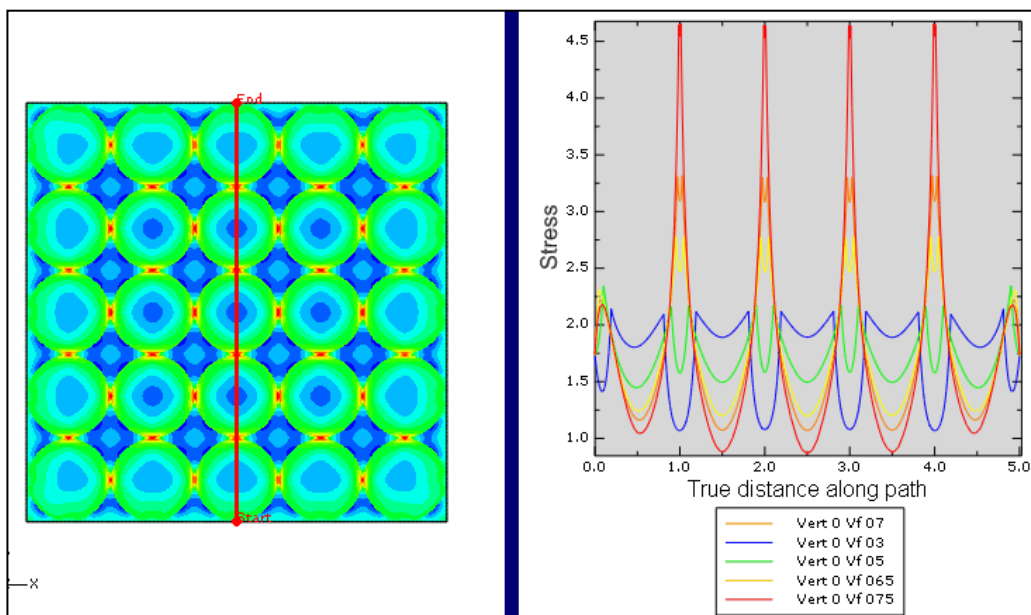


Figure 8: Vertical section at the center.

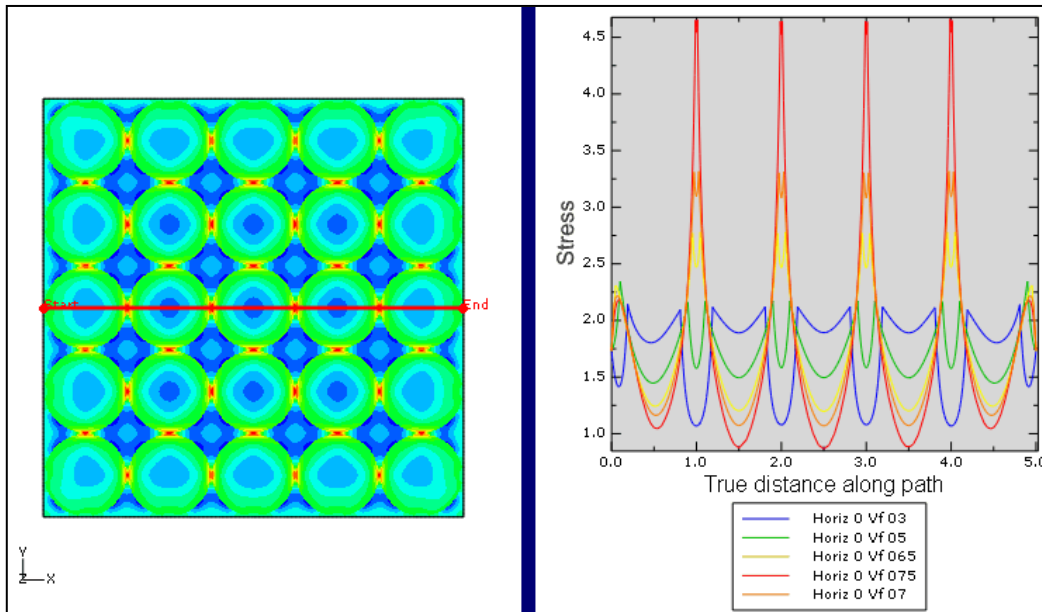


Figure 9: horizontal section at the center.

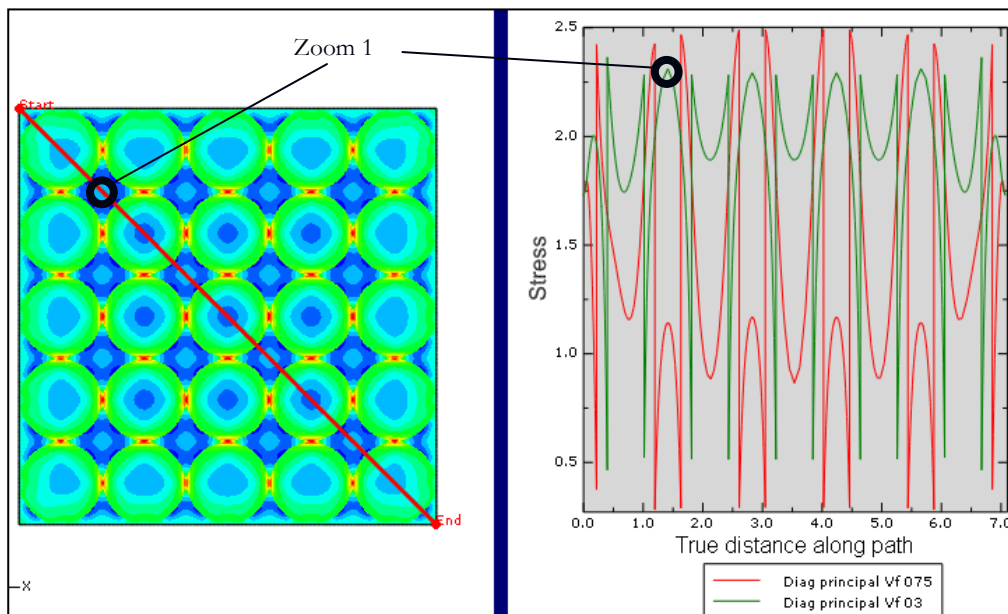


Figure 10: Main diagonal section.

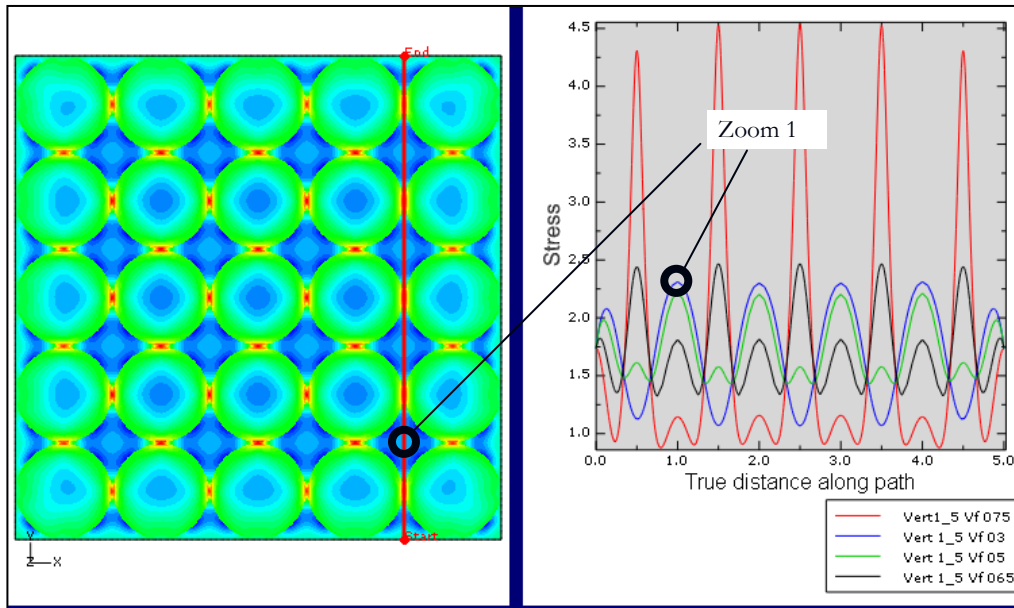


Figure 11: Vertical section at 1.5

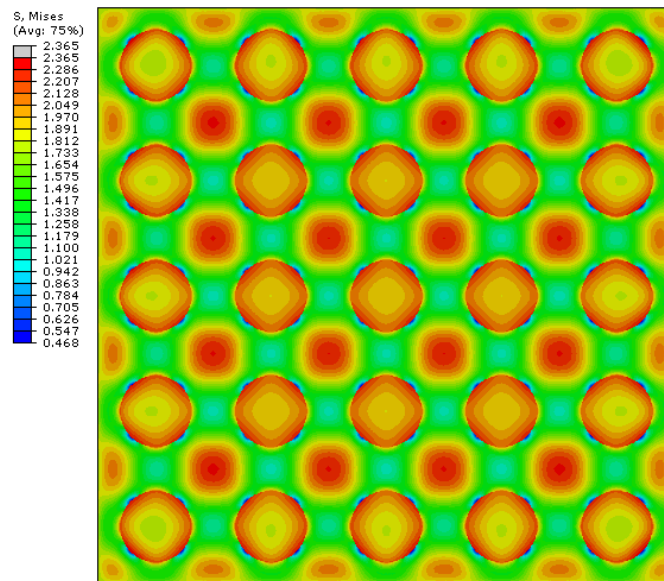


Figure 12: RVE, undamaged.

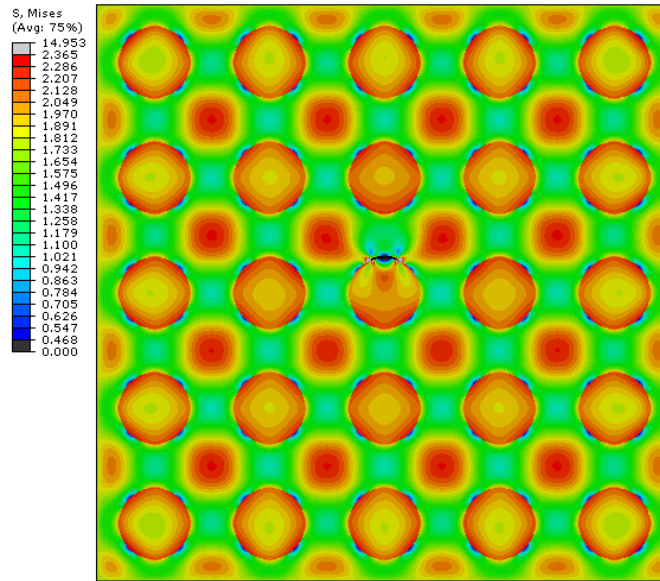


Figure 13: RVE, $V_f= 30\%$, damage extent=12.5%

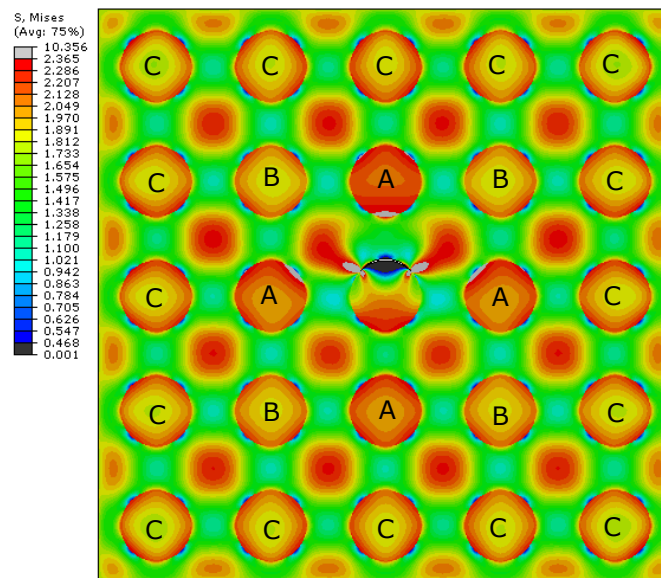


Figure 14: RVE with $V_f= 30\%$, damage extent=25%

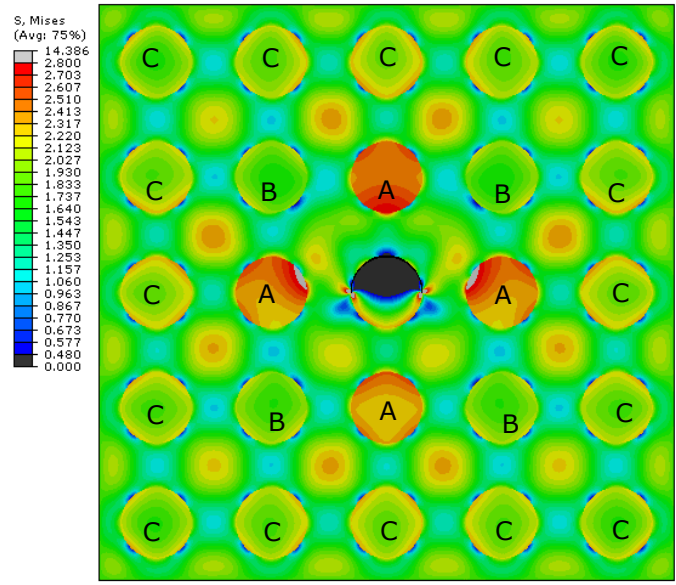


Figure 15: RVE with $V_f=30\%$, damage extent=50%. Stress scale: 2.8-0.48 Mpa.

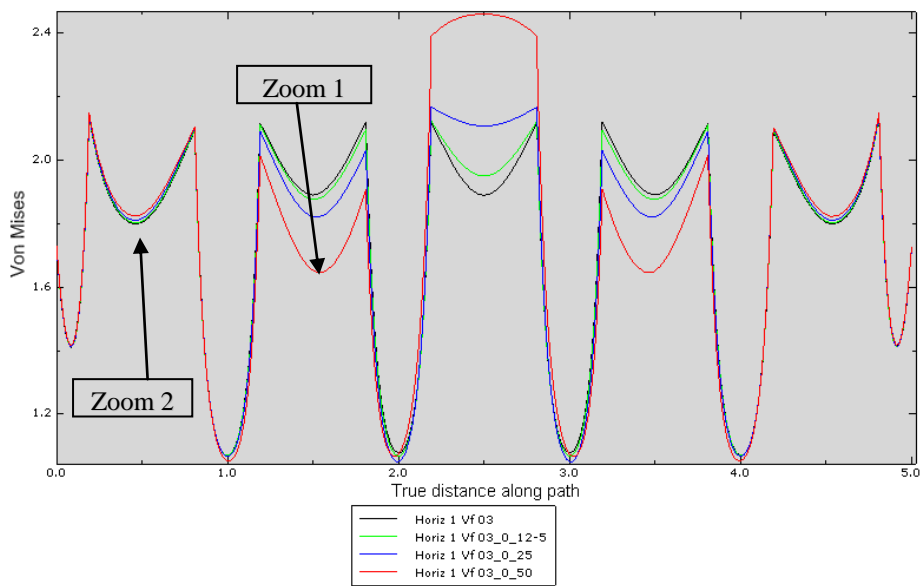


Figure 16: Plot of section identified in Figure 19.

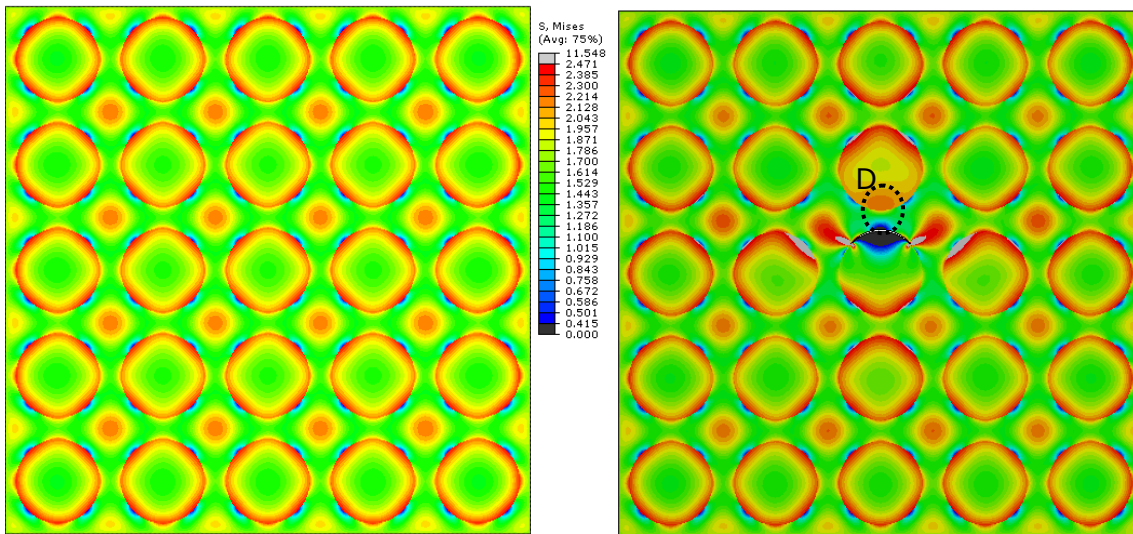


Figure 17: RVE with $V_f=50\%$ Left: undamaged. Right: damage extent: 25%.

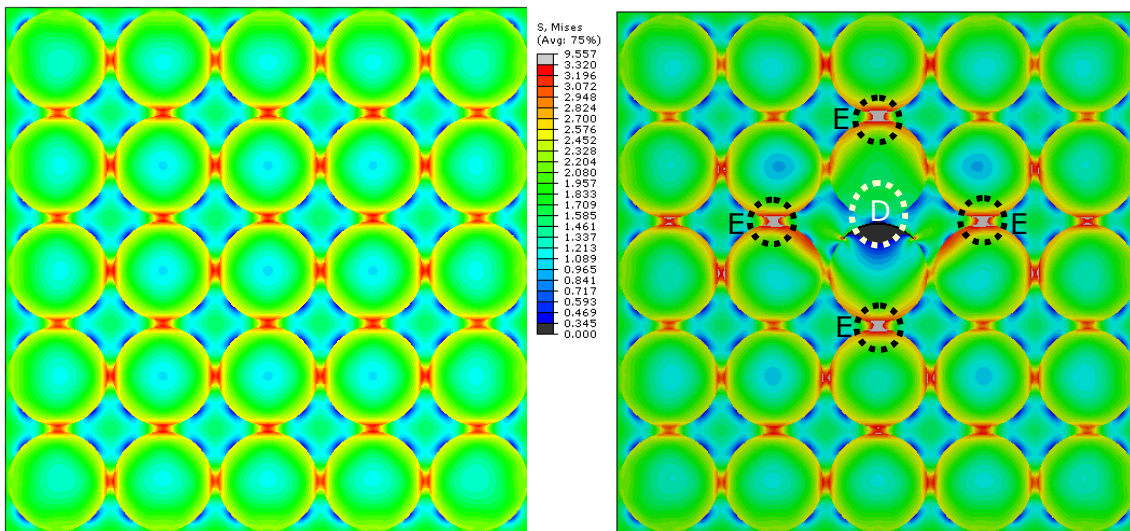


Figure 18: RVE with $V_f=70\%$ Left: undamaged. Right: damage extent: 25%.

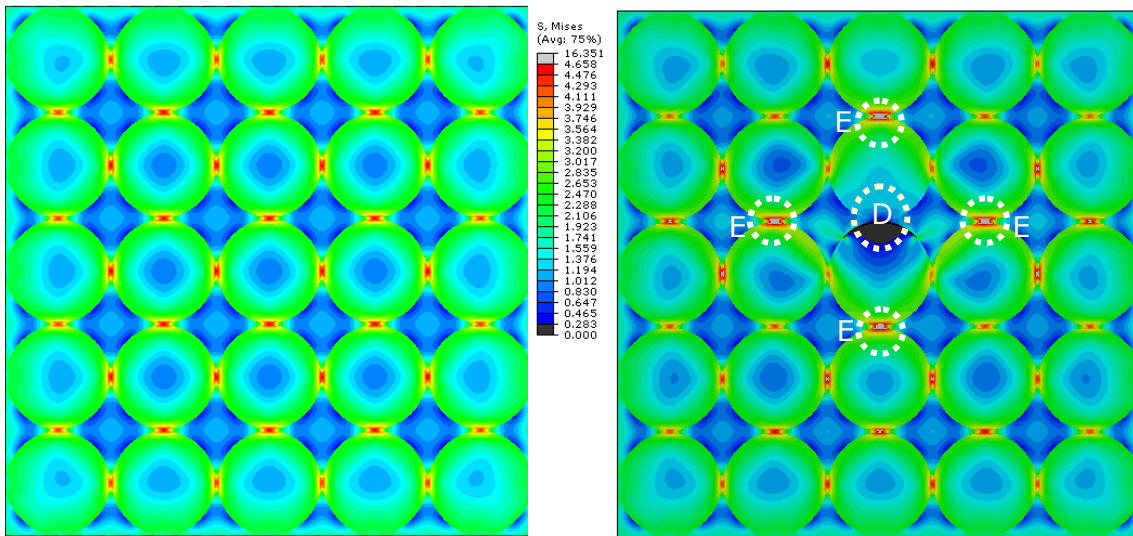


Figure 19: RVE with $V_f=75\%$ Left: undamaged. Right: damage extent: 25%.

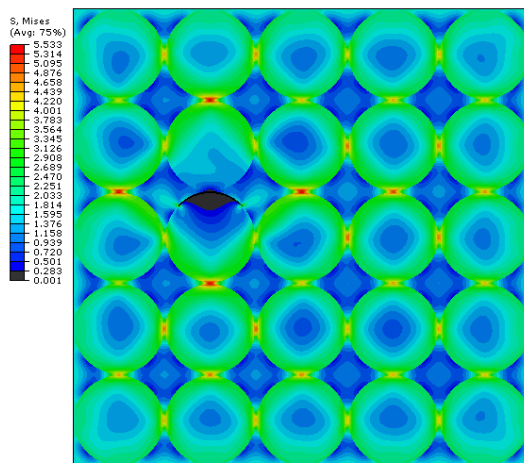


Figure 20: damage in one fiber.

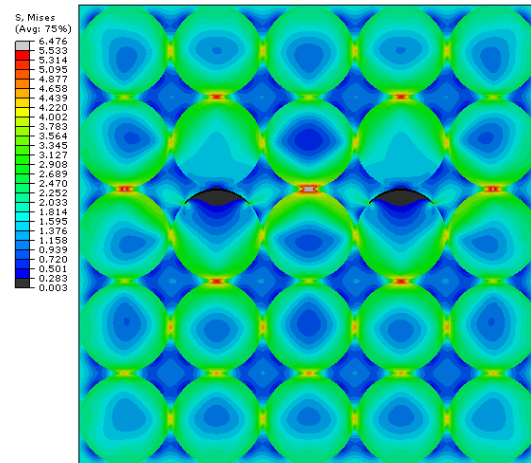


Figure 21: damage in two fibers.

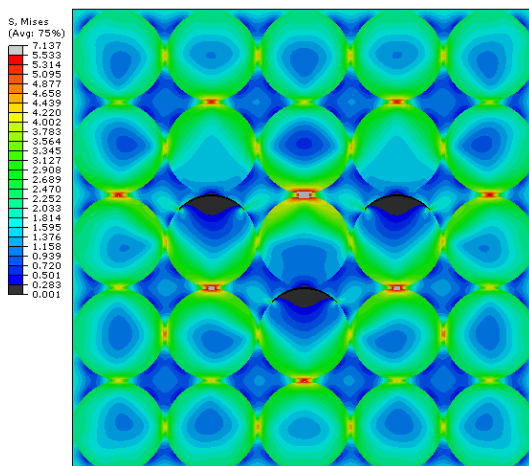


Figure 22: damage in three fibers.

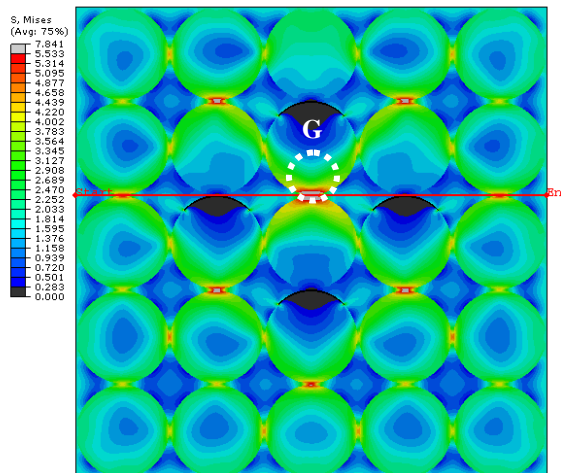


Figure 23: damage in four fibers.

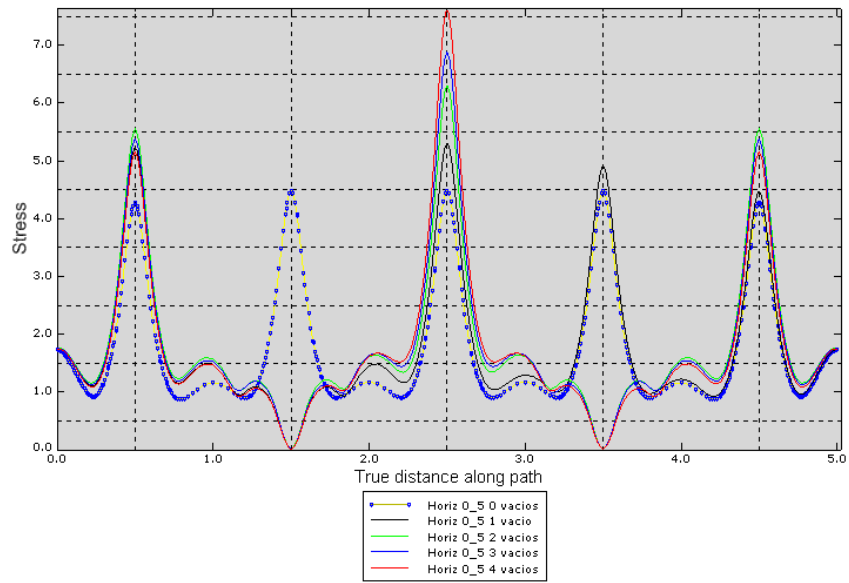


Figure 24: von Mises stresses at section “Horiz 0.5” in Figure 31.

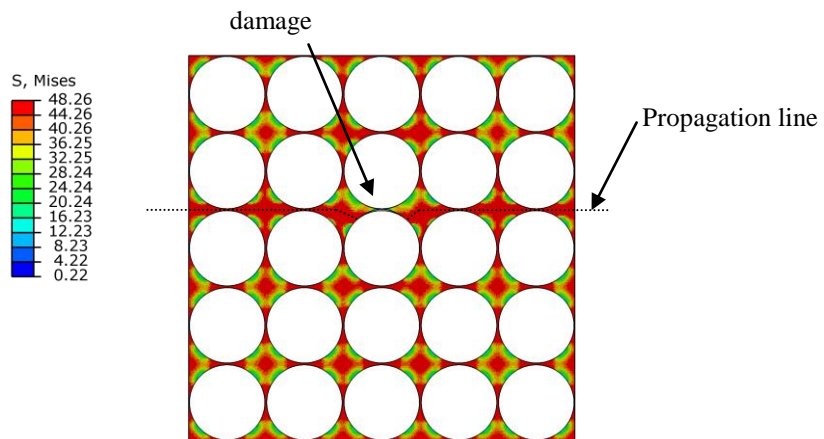


Figure 25: Load 55%

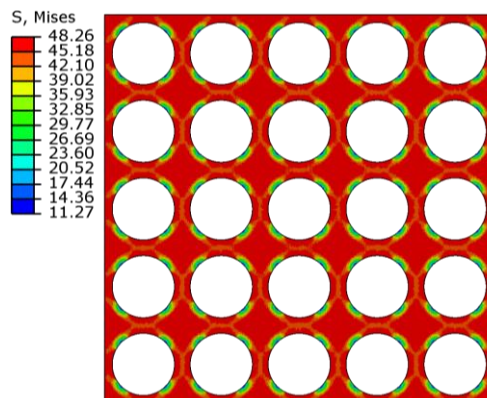


Figure 26: Plasticity with no damage

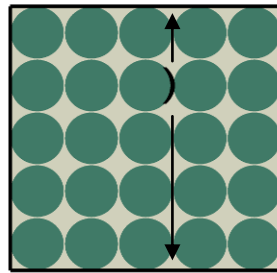


Figure 27: Yield propagation in the matrix.

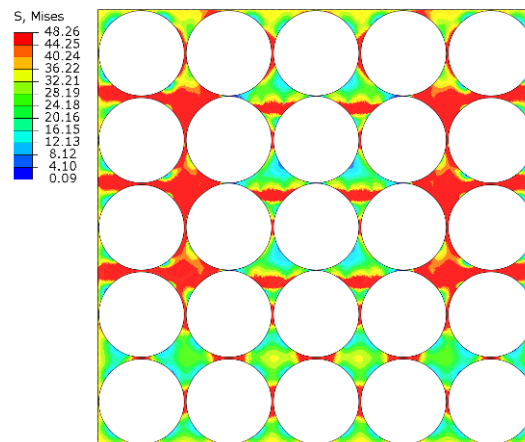


Figure 28: Propagation of nine voids in a RVE with $V_f=75\%$

REFERENCES

- ABAQUS v. 6.7, Dassault Systèmes, Providence, RI, US. 2009.
- Bonora, N., Ruggiero, A., Micromechanical modeling of composites with mechanical interface – Part II: Damage mechanics assessment, *Composites Science and Technology*, 66 (2):324-332, 2005.
- Caporale, A., Luciano, R., Sacco, E., Micromechanical analysis of Interfacial debonding in unidirectional Fiber-reinforced composites, *Computers & Structures*, 84 (31-31):2201-2210, 2006.
- Foulc, M.P., Bergeret, A., Ferry, L., Lenny, P., and Crespy, A., Study of hygro-thermal ageing of glass Fiber reinforced PET Composites. *Polymer Degradation and Stability*, 89 (3):462-469, 2005.
- Godoy, L. A., Modelos y Enfoques para problemas con acoplamiento de Micro y Macro Estructuras, *Mecánica Computacional*, 22:1964-1984, 2003.
- Godoy, L. A., Mondragón, V., Pando, M.A., Acosta, F.J., Comportamiento micro-mecánico de compuestos con micro-daño, *Mecánica Computacional*, 27:1253-1265, 2008.
- Jones, R., *Mechanics of composite materials*. Taylor and Francis, PA, 1999.
- Kajorncheappunngam, S., Rakesh. KG., GangaRao H.V. Effect of Ageing Environment on Degradation of Glass-Reinforced Epoxy, *Journal Composites of Construction*, 6 (1):61-69, 2002.
- Kaminski, M., *Computational Mechanics of Composites Materials*, London: Springer-Verlag,

2005.

- Kwon, Y., Study of damage evolution in composites using damage mechanics and micro-mechanics, *Composites structures*, 38 (1-4):133-139, 1997.
- Mondragon, M. V. *Modelo de la micromecánica de materiales compuestos considerando degradación higrotérmica*. Tesis de Maestría, Universidad de Puerto Rico, Mayaguez, 2008.
- Obando, J.C., Pando, M.A., Acosta, F.J., Godoy, L.A., Assessment at the Micro Level of the Hygrothermal Degradation of Fiber Reinforced Polymer Materials. *ASME International Mechanical Engineering*, Congress and Exposition, Lake Buena Vista, Florida, November 13-19, 2009.
- Ray, B.C. Temperature effect during humid ageing on interfaces of glass and carbon fiber reinforced epoxy composites, *Journal of Colloid and Interface Science*, 298 (1):111-117, 2005.
- Reifsnider, K.L., Modelling of the interphase in polymer-matrix composite material systems. *Constructions Industrielles*, 25 (7):462-469, 1994.
- Sevostianov, I., Verijenko, V., Verijenko, B., Evaluation of microstructure and properties deterioration in short fiber reinforced thermoplastics subjected to hydrothermal aging, *Composites Structures*, 62 (3-4):409-415, 2003.